frontiers | Frontiers in Marine Science

TYPE Original Research
PUBLISHED 04 August 2025
DOI 10.3389/fmars.2025.1648806

OPEN ACCESS

EDITED BY
Marco Bajo,
National Research Council (CNR), Italy

REVIEWED BY
Yi Shan,
Guangzhou University, China
Qinwen Du,
Chang'an University, China

*CORRESPONDENCE
Xing Xiao
xx_0524@126.com

RECEIVED 17 June 2025
ACCEPTED 17 July 2025
PUBLISHED 04 August 2025

CITATION
Wang Z, Lv N, Xiao X and Wu Q (2025) Experimental study on the dynamic shear modulus and damping ratio of structural soft soils from the Yangtze River floodplain considering consolidation degree. *Front. Mar. Sci.* 12:1648806. doi: 10.3389/fmars.2025.1648806

Experimental study on the dynamic shear modulus and damping ratio of structural soft soils from the Yangtze River floodplain considering consolidation degree

Zhijun Wang[1], Na Lv[2], Xing Xiao[3]* and Qi Wu[3]

[1]Huarun New Energy Investment Co., Ltd., Shenzhen, China, [2]Huadong Engineering Corporation Limited, Hangzhou, China, [3]Institute of Geotechnical Engineering, Nanjing Tech University, Nanjing, China

To explore the characteristics of the dynamic shear modulus of structural soft soil, undisturbed structural soft from the floodplain of the Yangtze River in Nanjing was subjected to strain-controlled cyclic triaxial tests to investigate how the initial effective confining pressure (σ'_m), consolidation ratio (k_c), and degree of consolidation (U) influence the maximum dynamic shear modulus G_{max} and dynamic shear modulus (G) and damping ratio (λ). The results show that for this soil, G decreases with increasing shear strain amplitude (γ), and for a given γ, G increases with increasing σ'_m, k_c, and U. Compared with soil from the Yangtze estuary, k_c has a greater effect on G_{max} of the floodplain structural soft soil. Finally, a modified Martin-Davidenkov model is proposed for predicting G/G_{max} of floodplain structural soft soil under different σ'_m, k_c, and U.

KEYWORDS

structural soft soil, dynamic shear modulus, damping ratio, initial static stress, degree of consolidation

1 Introduction

Structured soft soils, as typical depositional products formed under specific geological and environmental conditions, are widely distributed in floodplains, deltaic regions, and coastal lowlands (Tankiewicz, 2016; Bucci et al., 2018; Boulanger and DeJong, 2018; Beyzaei et al., 2020). Their characteristic interbedded structure – consisting of alternating layers of silt, clay, and occasionally fine sand – typically ranges from centimeters to meters in thickness, resulting in pronounced spatial heterogeneity, weak interlayer interfaces, and complex hydro-mechanical interactions. In modern geotechnical engineering, such stratified deposits pose significant challenges: when serving as subgrades for high-speed railways or expressways, differential compressibility between layers may induce uneven

settlement; when acting as bearing strata for large storage tanks or wind turbine foundations, cyclic loading can trigger interfacial slip and cumulative deformation; in deep excavation projects, the sand – clay alternation may lead to elevated risks of groundwater-induced seepage failures. In addressing these critical engineering concerns, the study of soil stiffness and damping parameters plays a central role. The initial shear modulus fundamentally governs the accuracy of settlement prediction and informs differentiated foundation design strategies. Meanwhile, the nonlinear characteristics of modulus degradation and damping evolution under cyclic loading control the fatigue performance of foundations and strongly influence the clay layers' capacity to inhibit sand liquefaction. Quantitatively characterizing the modulus-damping behavior of structured soft soils thus provides an essential theoretical basis for settlement mitigation, vibration attenuation, and anti-liquefaction design. Moreover, it establishes a vital parameter framework supporting intelligent construction, digital monitoring, and lifecycle performance assessment of major infrastructure projects in transportation, energy, and water resources.

Numerous researchers have investigated the static and dynamic properties of structural soft soils through various experimental methods (Liu et al., 2021; Jin et al., 2022; Zhuang et al., 2022; Liu and Xue, 2022; Shan et al., 2024; Xiao et al., 2025). Tankiewicz (2015) performed static triaxial tests on such soils and reported distinct strength anisotropy, along with significant variation in failure patterns and shear strength among samples. The permeability and anisotropic shear strength of interbedded soils were found to exceed those observed in many conventional soil types. Wichtmann and Triantafyllidis (2017) compiled a dataset comprising around 60 monotonic and cyclic triaxial tests to investigate how factors such as consolidation stress, strain rate, initial stress ratio, and stress amplitude affect the mechanical response of clay. Ma et al. (2019) conducted ring shear tests on remolded, overconsolidated soft interlayers, examining the effects of initial water content and applied consolidation stress under drained conditions. Their findings revealed that an increase in water content leads to a reduction in shear strength, with cohesion being more susceptible to moisture changes than the internal friction angle. Additionally, consolidation stress was identified as a key factor governing whether the material exhibited strain-softening or strain-hardening behavior. Through extensive cyclic triaxial tests, Duong et al. (2016) analyzed how moisture and fines content influence the resilient modulus of structural soft soils obtained from a railway subgrade in France. They concluded that under unsaturated conditions, soils with elevated fines content tend to develop a higher resilient modulus due to the reinforcing effect of capillary suction. Xiao et al. (2024) systematically analyzed the stiffness degradation and flow characteristics of marine clay under cyclic loading. Based on cyclic simple shear tests conducted on undisturbed samples from three offshore sites, they quantified the stiffness degradation index (δ) and the average flow coefficient (κ) under varying plasticity index (I_P) and cyclic stress ratio (CSR) conditions. Furthermore, a δ prediction model incorporating I_P and CSR was developed, and a unified relationship $\kappa/\kappa_f \sim \delta$ was proposed, revealing a stable negative exponential correlation between the two parameters.

In practice, the *in-situ* soils are often not fully consolidated at the time of construction, owing to factors such as fluctuating groundwater levels and limited consolidation time. As a result, soil layers with different degrees of consolidation (U) are commonly encountered. The mechanical behavior of such partially consolidated soft soils under cyclic loading (e.g., due to earthquakes, traffic, or wave actions) can differ significantly from that of fully consolidated soils. However, conventional dynamic design approaches usually assume full consolidation, which may lead to inaccurate predictions of deformation, stiffness degradation, or even failure risks. Therefore, a better understanding of how the degree of consolidation affects the dynamic properties of soft soils is essential for improving seismic safety evaluations and optimizing geotechnical design in such challenging ground conditions. The degree of consolidation (U) is a key parameter for assessing the consolidation state of soil, as it directly influences its load-bearing capacity and deformation behavior. For instance, in bridge construction, it is essential to evaluate the U value of the riverbed soil to ensure it can adequately support the bridge structure. Incorporating U into testing protocols can significantly reduce the time required for consolidation, thereby enhancing experimental efficiency. The degree of consolidation of a soil sample can be represented by U. In laboratory testing, U is defined as the ratio of the specimen's displacement at a given moment under a specified consolidation pressure to its final consolidation displacement (Wang et al., 2025).

$$U = \frac{S_t}{S_\infty} \tag{1}$$

In Equation 1, U represents the consolidation degree under a given pressure level; S_t is the displacement required to reach a certain U; and S_∞ is the maximum displacement under that pressure level. S_∞ is defined as the final displacement when the average strain rate falls below 1×10^{-3}%/min(Wang et al., 2025).

To date, studies on the influence of U on the cyclic response characteristics of clay remain limited. Chu and Yan (2005) demonstrated that different values of U can be achieved by manipulating pore water pressure and settlement behavior. Similarly, Lim et al. (2006) prepared soft clay samples with various Us by regulating pore pressure dissipation, and observed notable differences between clay with low U and normally consolidated clay. Hirao and Yasuhara (1991) obtained samples with different consolidation levels by adjusting the consolidation duration. Building upon these foundational efforts, some scholars have begun exploring the mechanical behavior of clay under low consolidation states. For instance, Wang et al. (2019) employed dynamic triaxial testing to examine the post-cyclic shear response of reconstituted marine silty clay with different reconsolidation degrees. Their results showed that the critical stress line is influenced by the amplitude of prior cyclic loading. Additionally, Zhu et al. (2022) conducted cyclic consolidation experiments on marine soft clay with varying U values, determined the critical cyclic stress ratios (CSRs), and developed a

permanent strain prediction model incorporating both *CSR* and *U*. Zheng et al. (2024) used a range of monotonic and cyclic tests on under-consolidated marine soft clay using a cyclic triaxial apparatus. By comparing with normally consolidated soils, they analyzed the development pattern of cumulative strain with a range of consolidation degrees (U = 0.5 to 1). Wang et al. (2025) performed a series of cyclic simple shear tests on reconstituted marine soft clay under different consolidation degrees and cyclic stress ratios (*CSR*s). Their results demonstrated that cyclic shear strength increases with the consolidation degree *U*; specimens with higher *U* require greater *CSR* to reach failure. Moreover, at a given *CSR*, higher *U* specimens tended to undergo predominantly elastic deformation with limited strain, whereas lower *U* samples showed a mix of elastic and plastic deformation, accompanied by more severe softening. Despite foundational work on the effect of consolidation degree (U) on soil properties, research into the behavior of clays under low or varying *U* remains at an early stage. Most studies have focused on theoretical models and monotonic soil behavior, leaving the complex, strain-dependent, and hysteretic characteristics of such soils less explored. This study fills this gap by investigating the dynamic shear modulus and damping ratio of soft soils under varying degrees of consolidation, specifically under different initial consolidation conditions. By analyzing how consolidation interacts with factors such as initial confining pressure and consolidation ratio in floodplain soils, our research offers new insights into the behavior of these soils under partial consolidation. The novelty of our work lies in the systematic examination of these interdependencies and the development of an empirical framework for predicting the nonlinear behavior of soft soils under different initial consolidation conditions. This study makes a significant incremental contribution to the understanding of soil dynamics in geotechnical engineering, especially in environments with fluctuating consolidation conditions.

To clarify how these key factors jointly influence the stiffness degradation and strain-dependent behavior of structural soft soils under cyclic loading, this paper investigates the characteristics of the dynamic shear modulus (G) of soft clay in the floodplain of the Yangtze River under different values of the initial effective confining pressure (σ'_m), consolidation ratio (k_c), and degree of consolidation (U). The results aim to improve understanding of the nonlinear dynamic response of soft soils with structural features, provide reference data for geotechnical seismic design, and contribute to more efficient laboratory testing procedures by incorporating consolidation degree as a meaningful parameter.

2 Test program and procedures

2.1 Test material

The specimens used in this study were all collected from construction sites in Jiangbei New District which were obtained through thin-wall Shelby tube sampling during site investigation drilling. To minimize sample disturbance, the tubes were hydraulically pushed into the soil layer at a constant rate without rotation. After retrieval, each tube was carefully sealed with paraffin wax and plastic film to preserve natural water content and structural integrity. The sealed samples were transported in an upright position and stored at low temperature to prevent desiccation or structural change before laboratory testing. Prior to testing, visual inspection and trimming were conducted to select intact segments for specimen preparation. This ensured that the soil structure remained as close as possible to *in-situ* conditions throughout the testing process. and are representative of the typical soft clay of the Yangtze River floodplain facies. The undisturbed Yangtze River floodplain facies soft clay appears gray-brown in color, with distinct horizontal bedding and interbedded sandy layers, as shown in Figure 1. After air-drying, disaggregation, and preliminary sieving, the undisturbed soil becomes a loose granular material. Particle size distribution tests reveal that, apart from a small amount of fine sand, most of the particles are smaller than 0.075 mm after oven-dried sieving. This indicates that the floodplain facies soft clay is mainly composed of clay minerals and fine detritus smaller than silt grade. Figure 1 presents scanning electron microscope (SEM) images of the Yangtze River floodplain facies soft clay. At the microscopic level, the undisturbed clay mainly appears as aggregated flocculent or platy structures, with loosely stacked clay particles often forming lamellar arrangements on their surfaces. In addition to these clay aggregates, numerous angular

FIGURE 1
Undisturbed Yangtze River floodplain facies soft soil and particle composition. **(a)** Undisturbed stratified structure, **(b)** Disturbed dry soil particles, **(c)** Scanning electron microscope image.

and irregularly shaped silt particles are observed. As for inter-aggregate connections, these clusters or particles are bound either through direct contact or by cementitious substances, predominantly forming edge-to-face or point-to-face contacts. Due to prolonged fluvial transport during its deposition, this soft clay is highly dispersive and strongly hydrophilic, resulting in high water content and large void ratios. It generally shows high compressibility and sensitivity, along with typical characteristics such as creep and thixotropy. Mineralogical analysis further reveals a relatively simple clay mineral composition, dominated by illite (~70%) and chlorite, with detrital minerals mainly consisting of quartz and feldspar. The overall material composition is relatively homogeneous.

2.2 Testing apparatus and principles

Strain-controlled staged cyclic triaxial tests were conducted using the HCA-300 multifunctional cyclic triaxial apparatus developed by GCTS (Figure 2). This advanced testing system is capable of performing both conventional triaxial tests and torsional shear tests with synchronously coupled bidirectional dynamic loading, allowing simulation of various types of loads such as seismic, traffic, and wave-induced loads. The main technical specifications of the triaxial system used in this study, including controller parameters, sensor ranges, accuracy, and measurement deviations, are summarized in Table 1. See (Chen et al., 2019) for more details about the HCA-300 system.

According to elastic theory, the shear stress τ and shear strain γ on the 45° plane of the specimen during loading can be calculated using Equation 2:

$$\begin{cases} \tau = \sigma_d/2 \\ \gamma = (1+\nu)\varepsilon \end{cases} \quad (2)$$

In Equation 2, ν denotes Poisson's ratio, for the *in situ* interbedded soil of the Yangtze River floodplain, we take $\nu = 0.42$ (Zhuang et al., 2020). We acknowledge that ν may evolve with increasing strain during cyclic shearing in practical conditions. The assumption of a constant ν was adopted for model simplicity, and it has been widely used in similar studies (Xiao et al., 2023). The calculation methods for G and γ in cyclic triaxial tests are illustrated in Figure 3. In the equivalent linear viscoelastic constitutive model, the soil is regarded as a viscoelastic material. G is represented by the slope of the line connecting the peak points at both ends of the soil's hysteresis loop, while λ is related to the energy dissipation and elastic strain energy of the soil.

TABLE 1 The main technical indicators of HCA-300 dynamic triaxial instrument.

Controller	Capacity	Precision	Deviation
Axial loading frequency	20 Hz	–	–
Cell/Back presssure frequency	10 Hz	–	–
Axial force	4 kN	1 N	0.1% FS
Axial displacement	± 7 mm	5 μm	0.1% FS
Cell/Back pressure	1.0 MPa	0.1 MPa	0.1% FS
Cell/Back volume	2000 mL/ 1000 mL	0.05 mL	0.1% FS
Pore pressure	1.0 MPa	0.1 MPa	0.1% FS

2.3 Test program

To investigate the variation characteristics of shear modulus (G) and damping ratio (λ) of interbedded clay-sand soils with respect to consolidation degree (U), a series of strain-controlled cyclic triaxial tests on undisturbed interbedded clay-sand soils were conducted. Undisturbed soft clay samples were selected to preserve the natural microstructure, stratification, and bonding characteristics of the floodplain soil, which play a critical role in its dynamic behavior. By keeping other conditions constant, five test conditions with different U and consolidation ratios (k_c) were designed. k_c was applied under drained conditions to ensure complete dissipation of pore water pressure. Ladd and DeGroot (2004) pointed out that the value of k_c generally ranges from 1.0 to 1.5. The chosen consolidation ratios (k_c = 1.0, 1.2, 1.4) are representative of the stress history and preloading conditions commonly encountered in soft clay foundations in engineering practice, such as surcharge preloading or excavation-induced stress changes. Table 2 presents the basic physical and mechanical properties of the floodplain soft soils from each borehole, as well as the specific test plans. Parameters such as density (ρ), water content (w), void ratio (e), were measured and showed in Table 2.

2.4 Experimental method

For the cyclic triaxial tests under different consolidation degrees, the experimental procedure can be divided into the following four steps: (1) Prepare standard-sized solid cylindrical specimens from undisturbed soft soil samples and fully saturate them; (2) Mount the specimen onto the base of the testing apparatus, connect the top to the displacement sensor and loading system, and seal the pressure chamber; (3) After installation, apply confining pressure and deviator stress to the specimen according to the test conditions to achieve various degrees of consolidation. Consolidation is considered complete once the target degree of consolidation is reached; (4) Subject the specimen to strain-controlled staged cyclic loading, with shear strain amplitude gradually increasing from 1×10^{-5} to 1×10^{-2}. This strain range was chosen based on typical working strain levels observed in soft soil foundations in engineering practice (Wong et al., 2022). Each loading stage consists of five cycles at a frequency of 0.1 Hz.

2.5 Method for controlling consolidation degree

By normalizing the measured consolidation displacement curves of Yangtze River floodplain soft soil specimens under

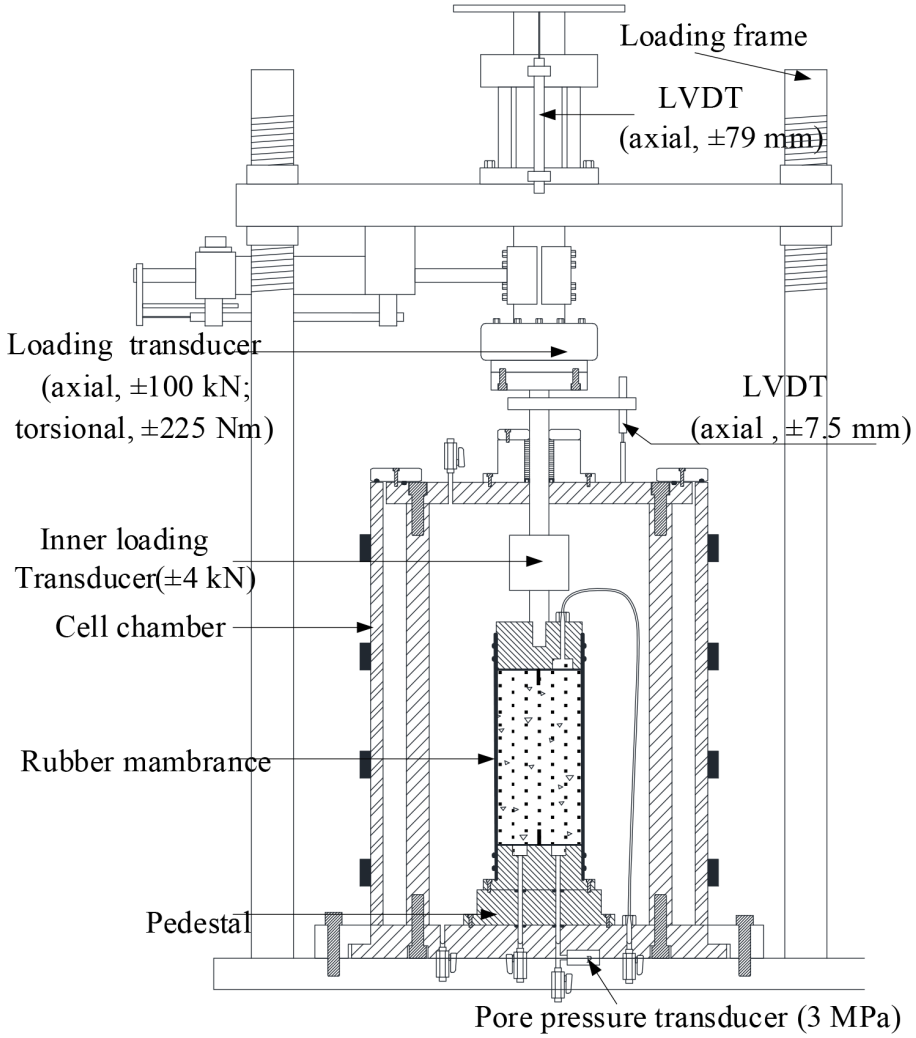

FIGURE 2
HCA-300 cyclic triaxial tester and schematic diagram.

different consolidation conditions (as shown in Figure 4), the variation curves of U with time were obtained, as illustrated in Figure 5. It can be observed that U of the floodplain soft soils exhibits a similar trend over time under different initial static stress conditions. Consequently, U can be expressed as a function of consolidation time t. the relationship between U and t was fitted using an exponential function in the following form:

$$U = 1 - ke^{-bt} \tag{3}$$

In Equation 3, k and b are shape parameters of the curve. The fitting results indicate that (Equation 3) provides a good fit for the floodplain soft soils of the Yangtze River. Therefore, this method is adopted in the present study to control U. Figure 5 presents the reference ranges of consolidation time corresponding to different U. This approach accounts for the potential errors between the fitted curve and the measured data. It can be observed that as the consolidation degree decreases, the time required for specimen consolidation is significantly reduced. The fitted curves do not pass through the origin because of the inherent structural characteristics of the soil.

3 Test results and analysis

3.1 Effect of U on Strain-dependent G and λ

Figure 6 presents the test results of the dynamic shear modulus (G) and damping ratio (λ) of undisturbed floodplain facies soft clay over a wide strain range under different degrees of consolidation. As shown in the Figure, at a given U, all types of floodplain facies soft clay exhibit a typical trend where G decreases with increasing shear strain amplitude (γ), while the damping ratio λ increases with γ. Furthermore, it can be observed that under the same γ, G increases significantly with increasing U, whereas the λ shows a slight decrease. This indicates that a higher U values correspond to

10.3389/fmars.2025.1648806

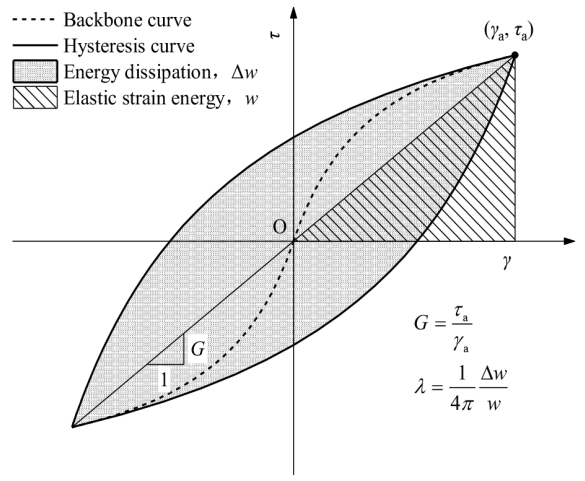

FIGURE 3
Equivalent linear dynamic viscoelastic constitutive model.

more complete dissipation of excess pore water pressure and further consolidation settlement, which tends to preserve or enhance the existing soil fabric and interparticle contacts in undisturbed samples. Comparisons among Figures 6a-c further reveal that the influence of U on G becomes more pronounced with increasing initial effective confining pressure. This suggests that the effect of U on G of floodplain facies soft clay is correlated with σ'_m. Similarly, by comparing Figures 6b-e, it can be seen that as the consolidation ratio k_c increases, the influence of U on G also becomes more significant. This indicates that G of floodplain facies soft clay is not only affected by the U but also closely related to the k_c.

3.2 Effect of U on maximum dynamic shear modulus G_{max}

The maximum G_{max} is the dynamic shear modulus when the strain percentage is less than 10^{-5}, in which case the soil is considered to be in a purely elastic state. And so in this study G_{max} was obtained using the extrapolation method at 0.0001% strain (Hardin and Drnevich, 1972). Figure 7 illustrates the variation trend of G_{max} of the Yangtze River floodplain soft soil with U. As shown in Figures 4 and 5, G_{max} increases with increasing U under different consolidation conditions, and the two exhibit an exponential correlation. This indicates that G_{max} of the undisturbed Yangtze River floodplain soft soil is influenced not only by the initial effective confining pressure and the consolidation ratio k_c, but also by U.

TABLE 2 Basic physical properties and test cases of soil samples.

Sample ID	H/m	ρ/g•cm^{-3}	w/%	e	w/%	σ_m'/kPa	k_c	U
C-50-1.0-0.6	6.0-6.1	1.70	41.08	1.12	17.4	50	1.0	0.6
C-50-1.0-0.8	6.1-6.2	1.73	40.11	1.10	17.2	50	1.0	0.8
C-50-1.0-0.95	6.2-6.3	1.74	39.55	1.09	17.5	50	1.0	0.95
C-50-1.0-1.0	6.3-6.4	1.71	41.45	1.13	17.3	50	1.0	1.0
C-100-1.0-0.6	13.0-13.1	1.75	40.21	1.12	16.7	100	1.0	0.6
C-100-1.0-0.8	13.1-13.2	1.71	39.59	1.16	16.9	100	1.0	0.8
C-100-1.0-0.95	13.2-13.3	1.73	40.50	1.09	17.6	100	1.0	0.95
C-100-1.0-1.0	13.3-13.4	1.75	39.33	1.13	17.8	100	1.0	1.0
C-150-1.0-0.6	20.0-20.1	1.75	40.14	1.13	17.8	150	1.0	0.6
C-150-1.0-0.8	20.1-20.2	1.73	39.82	1.14	17.1	150	1.0	0.8
C-150-1.0-0.95	20.2-20.3	1.77	41.43	1.12	17.5	150	1.0	0.95
C-150-1.0-1.0	20.3-20.4	1.70	41.66	1.18	17.0	150	1.0	1.0
C-100-1.2-0.6	13.5-13.6	1.75	40.21	1.12	16.7	100	1.2	0.6
C-100-1.2-0.8	13.6-13.7	1.74	38.65	1.07	16.3	100	1.2	0.8
C-100-1.2-0.95	13.7-13.8	1.75	40.52	1.11	16.8	100	1.2	0.95
C-100-1.2-1.0	13.8-13.9	1.77	40.60	1.26	16.7	100	1.2	1.0
C-100-1.4-0.6	13.9-14.0	1.79	40.42	1.01	16.5	100	1.4	0.6
C-100-1.4-0.8	14.0-14.1	1.73	41.70	1.14	16.9	100	1.4	0.8
C-100-1.4-0.95	14.1-14.2	1.75	42.41	0.95	17.1	100	1.4	0.95
C-100-1.4-1.0	14.2-14.3	1.76	41.38	1.08	16.3	100	1.4	1.0

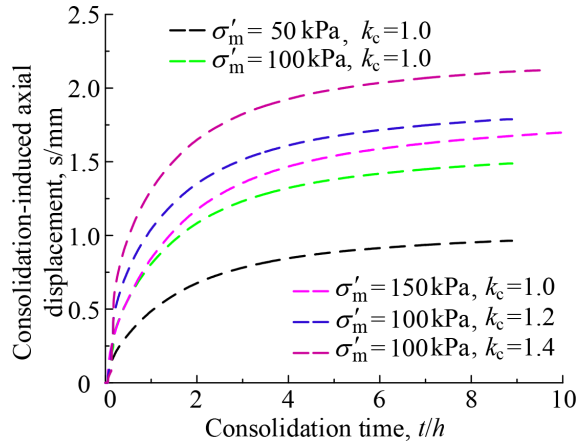

FIGURE 4
Consolidation displacement curves of soft soils in floodplain facies of the Yangtze River under different consolidation conditions.

Figure 7 also reveals that under isotropic consolidation conditions, the variation in σ'_m has a nearly identical effect on the growth rate of G_{max} with respect to U for the floodplain soft soil. Similarly, under the same σ'_m, the influence of k_c on the growth rate of G_{max} with increasing U is relatively minor. This indicates that the growth rate of G_{max} with U is not significantly affected by differences in σ'_m or k_c. Therefore, the relationship between G_{max} and U for floodplain soft soils under various initial consolidation conditions can be fitted using Equation 4:

$$G_{max} = A_1 \cdot U^k \tag{4}$$

The corresponding fitting parameters, as well as the experimental results, are summarized in the Table 3 below, where A_1 and k denote the fitting parameters. It can be observed that the values of G_{max} at $U = 1$ obtained from the experiments under different σ'_m or k_c conditions are very close to the fitted parameter A_1 and therefore we approximate that A_1 is numerically equal to G_{max} when $U = 1$. Moreover, the stress index k characterizes the influence of U on the growth rate of G_{max}. Regression analysis shows that the value of k is approximately 0.5. therefore, we adopted $k = 0.5$ in our derivation.

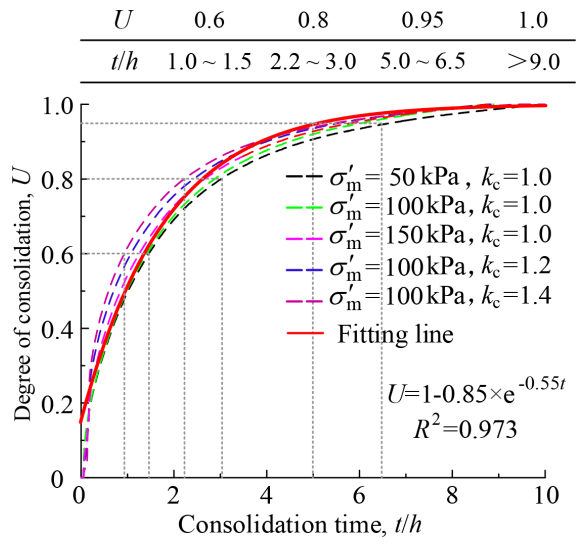

FIGURE 5
Consolidation curve and fitting of Yangtze River floodplain soft soil under different consolidation conditions.

To facilitate the empirical estimation of G_{max} for floodplain soft soils under different U, the value of G_{max} corresponding to a specific U is denoted as $G_{max,u}$, while the value under full consolidation (i.e., $U = 100\%$) is denoted as $G_{max,100\%}$. Accordingly, (Equation 5) can be rewritten in the following form:

$$G_{max,u} = \mu \cdot G_{max,100\,\%} \tag{5}$$

In this equation, μ represents the reduction factor of G_{max} under partial consolidation. Table 4 provides the reduction factors μ corresponding to different U for floodplain soft soils along the Yangtze River, which can serve as a reference for engineering practice.

3.3 Expressions of G/G_{max} and λ and parameters

To investigate the nonlinear and hysteretic characteristics of floodplain soft soils along the Yangtze River, the G/G_{max} and λ were fitted using the Martin-Davidenkov model (Martin and Seed, 1983) (Equation 6) and the λ model proposed by (Chen et al., 2006), (Equation 7) respectively.

$$\frac{G}{G_{max}} = 1 - \left[\frac{(\gamma/\gamma_0)^{2\beta}}{1+(\gamma/\gamma_0)^{2\beta}}\right]^{\alpha} \tag{6}$$

$$\lambda = \lambda_{min} + \lambda_0 \times (1 - G/G_{max})^{\beta_1} \tag{7}$$

In the equations, α and β are fitting parameters. The reference shear strain γ_0 corresponds to the strain value at which G/G_{max} equals 0.5. λ_{min} represents the minimum damping ratio of the soil at very small strains, while λ_0 and β are shape parameters that define the form of λ curve.

As shown in Figure 8, U has a significant influence on the relationship curves of $G/G_{max} - \gamma$. At the same strain level, the G/G_{max} values of the Yangtze River floodplain soft soil increase with increasing U, while the λ decreases as U increases. This indicates that as U increases, the dynamic behavior of the soil gradually shifts from nonlinear to linear, accompanied by a reduction in hysteretic behavior. Furthermore, a comparison of Figures 8a-c shows that with increasing σ'_m, the influence of U on the $G/G_{max} - \gamma$ and $\lambda - \gamma$ curves becomes more pronounced. This suggests that the effect of U on the nonlinear and hysteretic characteristics of the floodplain soft soil is dependent on the σ'_m. Similarly, a comparison of Figures 8b-e reveals that as k_c increases, the influence of U on the $G/G_{max} - \gamma$ and $\lambda - \gamma$ curves also becomes more evident. This indicates that the effect of U on the nonlinear and hysteretic behavior of the floodplain soft soil is also related to k_c.

This study investigates the influence of U on G and λ of Yangtze River floodplain soft soils under different σ'_m and k_c, based on cyclic triaxial testing. The degradation curve of G/G_{max} is closely related to the

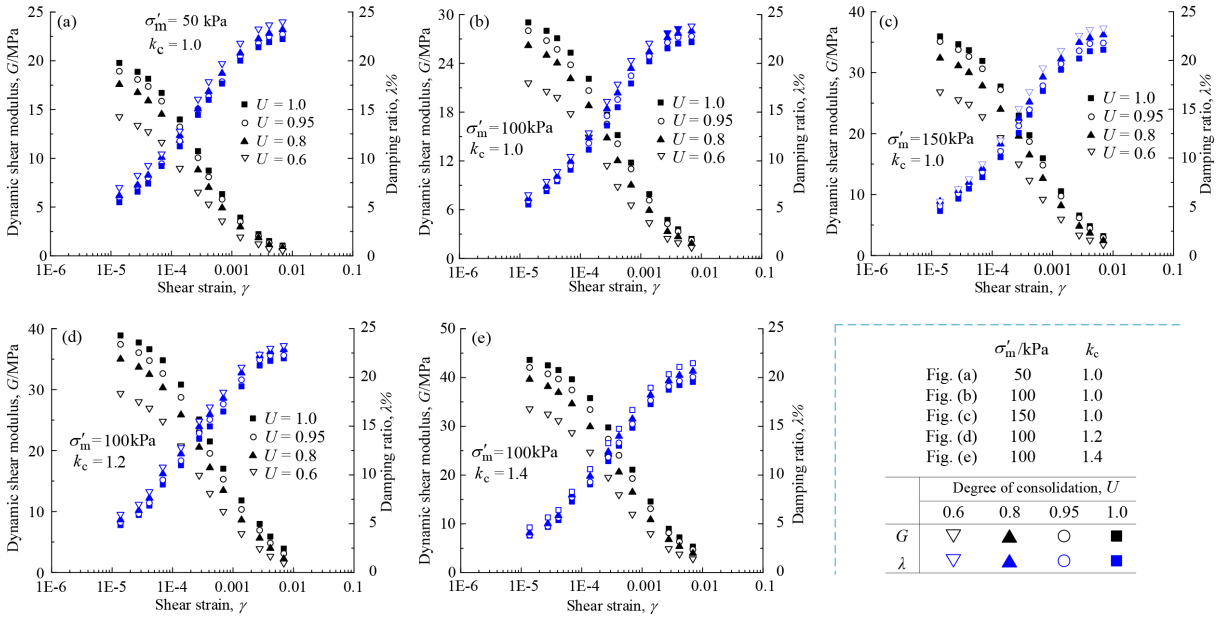

FIGURE 6
Test results of G and λ of Yangtze River floodplain soft soil with different Us. **(a)** σ'_m = 50 kPa, k_c = 1.0; **(b)** σ'_m = 100 kPa, k_c = 1.0; **(c)** σ'_m = 150 kPa, k_c = 1.0; **(d)** σ'_m = 100 kPa, k_c = 1.2; **(e)** σ'_m = 100 kPa, k_c = 1.4.

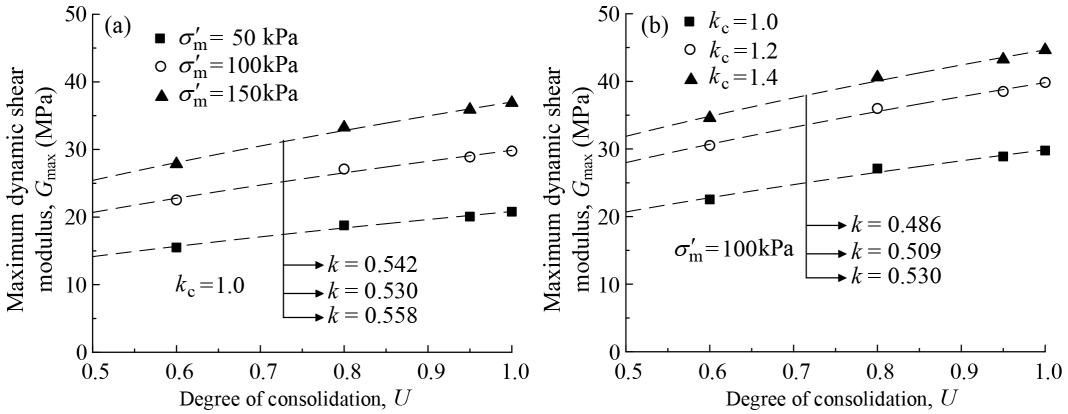

FIGURE 7
The relationship between the G_{max} of the Yangtze River floodplain soft soil and U. **(a)** The effects of σ'_m at k_c = 1.0; **(b)** The effects of k_c at σ'_m = 100 kPa.

TABLE 3 The summary table of fitted parameters for specimens under different σ'_m or k_c conditions.

k_c	σ'_m(kPa)	G_{max} when U equals 1.0 (MPa)	A_1	k
1.0	50	20.34	20.50	0.542
1.0	100	29.37	29.52	0.530
1.0	150	36.68	36.84	0.558
1.0	100	29.56	29.74	0.486
1.2	100	38.16	39.52	0.509
1.4	100	44.34	44.41	0.530

10.3389/fmars.2025.1648806

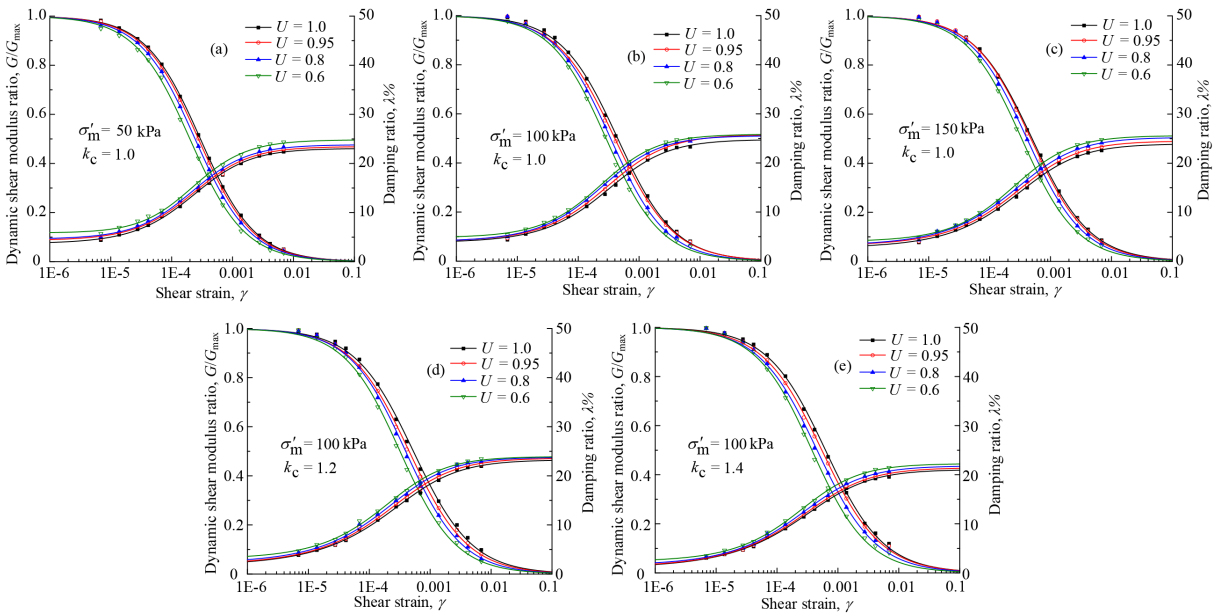

FIGURE 8
$G/G_{max} \sim \gamma$ and $\lambda \sim \gamma$ relationship curves of Yangtze River floodplain soft soils with different Us. **(a)** σ'_m = 50 kPa, k_c = 1.0; **(b)** σ'_m = 100 kPa, k_c = 1.0; **(c)** σ'_m = 150 kPa, k_c = 1.0; **(d)** σ'_m = 100 kPa, k_c = 1.2; **(e)** σ'_m = 100 kPa, k_c = 1.4.

$$\gamma_0' = \frac{\gamma_0}{\left[a + b\left(\frac{\sigma_m'}{P_a}\right)\right] \cdot (k_c)^c}$$

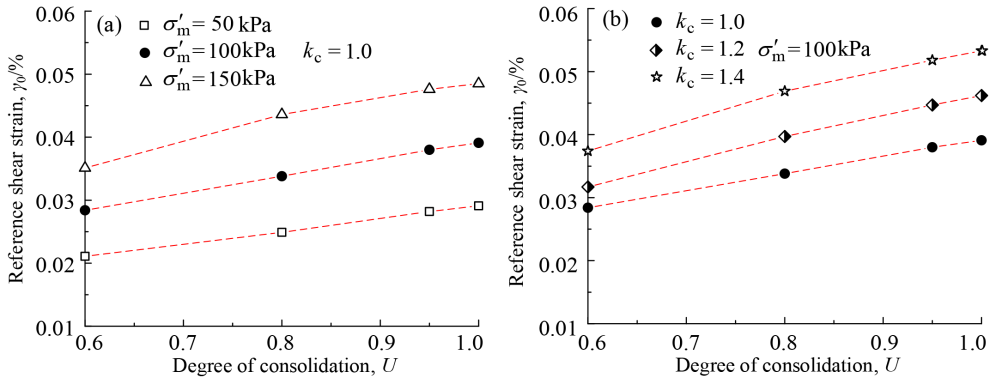

FIGURE 9
Relationships between U and γ_0 under different conditions of σ'_m and k_c. **(a)** The effects of σ'_m at k_c = 1.0; **(b)** The effects of k_c at σ'_m = 100 kPa.

three parameters in the Davidenkov model: α, β, and γ_0. Table 5 summarizes the values of these parameters under all test conditions. The results show that U has little effect on the parameters α and β. Therefore, when using the three-parameter Davidenkov model to fit the behavior of the floodplain soft soils, α and β can be reasonably taken as 1.0 and 0.47, respectively. In contrast, the reference shear strain γ_0 exhibits significant variability during nonlinear fitting, which may be associated with the variation in U under different test conditions.

TABLE 4 Reduction coefficient of G_{max} value under different degree of consolidation.

U	0.6	0.8	0.95
μ	0.75 ~ 0.78	0.88 ~ 0.90	0.97 ~ 0.98

Figure 9 shows the relationship curves between U and γ_0 under different σ'_m and k_c. It can be observed that when σ'_m and k_c are fixed, γ_0 increases significantly with increasing U. Moreover, as σ'_m and k_c increase, the influence of U on the rising trend of γ_0 becomes more

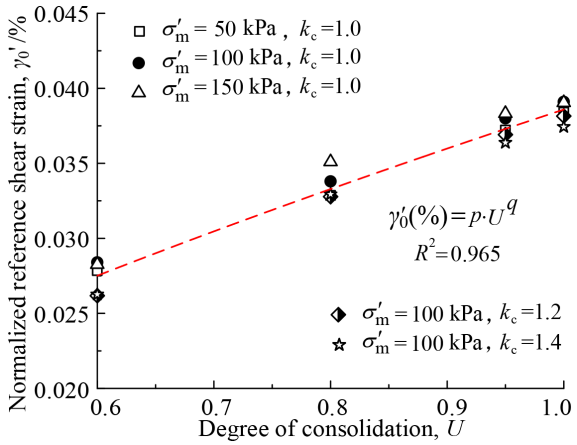

FIGURE 10
The relationship between U and the normalized reference shear strain γ_0'.

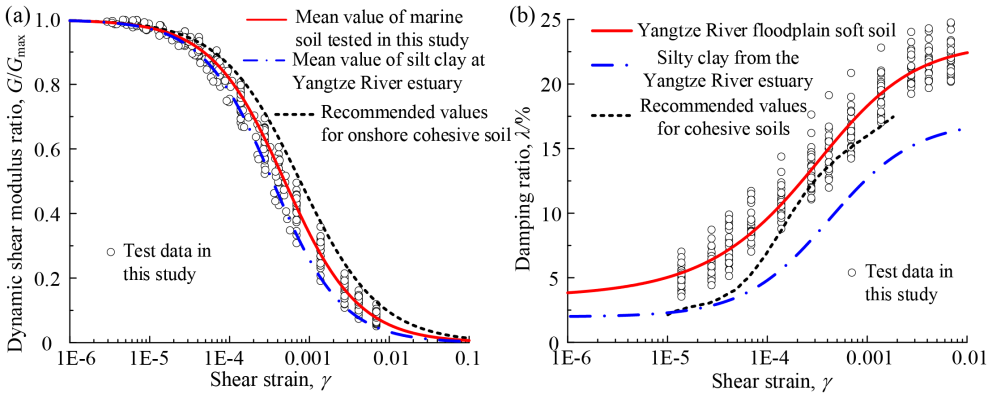

FIGURE 11
G/G_{max} ~ γ and λ~ γ relationship curves of different clay soils. **(a)** G/G_{max} ~ γ curves; **(b)** λ~ γ curves.

TABLE 5 Davidenkov model parameters for G/G_{max} ~ γ curve prediction.

Sample ID	α	β	γ_0(%)	Sample ID	α	β	γ_0(%)
C-50-1.0-0.6	0.998	0.480	0.0211	C-150-1.0-0.95	1.005	0.462	0.0476
C-50-1.0-0.8	1.000	0.480	0.0249	C-150-1.0-1.0	1.005	0.454	0.0485
C-50-1.0-0.95	1.000	0.482	0.0282	C-100-1.2-0.6	1.005	0.473	0.0317
C-50-1.0-1.0	1.001	0.481	0.0291	C-100-1.2-0.8	1.006	0.466	0.0397
C-100-1.0-0.6	1.005	0.477	0.0284	C-100-1.2-0.95	1.007	0.451	0.0447
C-100-1.0-0.8	1.005	0.472	0.0338	C-100-1.2-1.0	1.010	0.449	0.0462
C-100-1.0-0.95	1.005	0.451	0.0380	C-100-1.4-0.6	1.008	0.470	0.0374
C-100-1.0-1.0	1.006	0.462	0.0391	C-100-1.4-0.8	1.009	0.450	0.0469
C-150-1.0-0.6	1.004	0.474	0.0351	C-100-1.4-0.95	1.007	0.445	0.0518
C-150-1.0-0.8	1.004	0.462	0.0436	C-100-1.4-1.0	1.008	0.453	0.0533

In the specimen ID, the first number is the initial effective confining pressure σ_m', the second is the consolidation ratio k_c, and the third is the degree of consolidation U.

pronounced. As previously discussed, the σ'_m and k_c have a notable impact on the fitted parameters for floodplain soft soils. To further quantify the effect of U, the γ_0 under different initial static stress conditions is normalized. According to (Equation 8), γ_0 values under varying initial stress conditions can be normalized to γ'_0, which corresponds to a confining pressure of 100 kPa and a consolidation ratio k_c of 1.0.

$$\gamma_0^{'} = \frac{\gamma_0}{\left[a + b\left(\frac{\sigma'_m}{P_a}\right)\right] \cdot (k_c)^c} \tag{8}$$

The fitting results of γ'_0 under different U are shown in Figure 10. As illustrated in Figure 10, γ'_0 of various types of floodplain soft soils exhibits an increasing trend with rising U. Based on this observed pattern, an empirical relationship between γ'_0 and U can be established as Equation 9:

$$\gamma_0^{'} = p \cdot U^q \tag{9}$$

In Equation 9, p and q are fitting parameters, with values of 0.0386 and 0.66, respectively.

To further analyze the nonlinear and hysteretic behavior of Yangtze River floodplain soft soils, G and λ test data for silty clay from the Yangtze River estuary (σ'_m = 50 ~ 200 kPa) (Yang et al., 2019) were collected for fitting analysis. The fitting results for G/G_{max} and λ of the two clay types were compared with recommended and standard values for cohesive soils. The comparison results are shown in Figure 11. The recommended values were provided by (Sun et al., 2004). based on the average test data of conventional soils such as clay, silty clay, and silt from various regions across China. As shown in Figure 11a, the G/G_{max} – γcurves of Yangtze River floodplain soft soils generally fall within the statistical range of recommended and standard values for cohesive soils. Compared to the silty clay from the Yangtze estuary, the floodplain soft soils exhibit slower modulus degradation at large strains and relatively higher G/G_{max} values, indicating that their nonlinear behavior is weaker. Therefore, the empirical formula proposed in this study can be used to predict G/G_{max} for Yangtze River floodplain soft soils. As shown in Figure 11b, the λ of the floodplain soft soils shows considerable variability, which aligns with current understanding of damping behavior in cohesive soils. At small strain levels, the λ is relatively high, while at larger strains it approaches the recommended and standard values for cohesive soils, and is higher than the average λ of the estuary silty clay. Overall, the Yangtze River floodplain soft soils tend to exhibit higher λ, reflecting stronger hysteretic behavior.

4 Conclusion

The dynamic triaxial tests conducted in this study investigated the characteristics of dynamic shear modulus (G) and damping ratio (λ) of floodplain soft soils under different consolidation degrees. The analysis focused on how the maximum dynamic shear modulus (G_{max}), the degradation behavior of the normalized modulus ratio (G/G_{max}), and the growth trend of λ vary with consolidation degree (U). The main conclusions are as follows:

1. Under different initial static stress conditions, the U of floodplain soft soils along the Yangtze River shows a generally consistent trend with consolidation time. By fitting the relationship between U (defined by strain criteria) and consolidation time t, a method for estimating U based on time was established, along with corresponding reference durations.
2. Floodplain soft soils with varying consolidation degrees exhibit typical nonlinear and hysteretic behavior, characterized by low shear modulus and high damping ratio. As shear strain γ increases, G decreases while λ increases. Within different strain ranges, G increases with higher U, while λ decreases correspondingly.
3. G_{max} of Yangtze River floodplain soft soils is influenced by U, showing an increasing trend as U increases. Using the G_{max} value at full consolidation (U = 100%) as a reference, a range of reduction factors μ corresponding to different U is provided for practical reference.
4. The G/G_{max} – γcurves of undisturbed floodplain soft soils shift upward with increasing U, while the λ – γ curves shift downward, indicating that the dynamic behavior of the soil becomes more linear and less hysteretic as consolidation progresses. Compared to conventional cohesive soils, the floodplain soft soils of the Yangtze River exhibit more pronounced nonlinearity and stronger hysteretic characteristics.

Data availability statement

The original contributions presented in the study are included in the article/Supplementary Material. Further inquiries can be directed to the corresponding author.

Author contributions

ZW: Data curation, Writing – original draft, Visualization, Writing – review & editing, Validation. NL: Data curation, Writing – review & editing, Visualization. XX: Visualization, Methodology, Writing – review & editing. QW: Conceptualization, Writing – review & editing, Visualization.

Funding

The author(s) declare that no financial support was received for the research and/or publication of this article.

Conflict of interest

Author ZW was employed by the company Huarun New Energy Investment Co., Ltd. Author NL was employed by the company Huadong Engineering Corporation Limited.

The remaining authors declare that the research was conducted in the absence of any commercial or financial relationships that could be construed as a potential conflict of interest.

Generative AI statement

The author(s) declare that no Generative AI was used in the creation of this manuscript.

Publisher's note

References

Beyzaei, C. Z., Bray, J. D., Cubrinovski, M., Sarah, B., Mark, S., Mike, J., et al. (2020). Characterization of silty soil thin layering and groundwater conditions for liquefaction assessment. *Can. Geotech. J.* 57, 263–276. doi: 10.1139/cgj-2018-0287

Boulanger, R. W., and DeJong, J. T. (2018). Inverse filtering procedure to correct cone penetration data for thin-layer and transition effects. *Proc. Cone Penetration Testing*, 25–44.

Bucci, M. G., Villamor, P., Almond, P., Tuttle, M., Stringer, M., Ries, W., et al. (2018). Associations between sediment architecture and liquefaction susceptibility in fluvial settings: the 2010-2011 canterbury earthquake sequence, New Zealand. *Eng. Geol.* 237, 181–197. doi: 10.1016/j.enggeo.2018.01.013

Chen, G., Liu, X., Zhu, D., and Hu, Q. (2006). Experimental studies on dynamic soils in Nanjing. *Chin. J. Geotech. Eng.* 28, 1023–1027. doi: 10.3321/j.issn:1000-4548.2006.08.018

Chen, G. X., Zhao, D. F., Chen, W. Y., and Juang, C. H. (2019). Excess pore-water pressure generation in cyclic undrained testing. *J. Geotech. Geoenvironmental Eng.* 145, 04019022. doi: 10.1061/(ASCE)GT.1943-5606.0002057

Chu, J., and Yan, S. (2005). Estimation of degree of consolidation for vacuum preloading projects. *Int. J. Geomechanics* 5, 158–165. doi: 10.1061/(ASCE)1532-3641(2005)5:2(158

Duong, T. V., Cui, Y. J., Tang, A. M., Dupla, J. C., Jean, C., Nicolas, C., et al. (2016). Effects of water and fines contents on the resilient modulus of the interlayer soil of railway substructure. *Acta Geotech.* 11, 51–59. doi: 10.1007/s11440-014-0341-0

Hardin, B. O., and Drnevich, V. P. (1972). Shear modulus and damping in soils: design equations and curves. *Geotech. Spec. Publ.* 98, 667–692. doi: 10.1061/JSFEAQ.0001760

Hirao, K., and Yasuhara, K. (1991). Cyclic strength of underconsolidated clay. *Soils Foundations* 31, 180–186. doi: 10.3208/sandf1972.31.4_180

Jin, H., Guo, L., Sun, H., Shi, L., and Cai, Y. (2022). Undrained cyclic shear strength and stiffness degradation of overconsolidated soft marine clay in simple shear tests. *Ocean Eng.* 262, 112270. doi: 10.1016/j.oceaneng.2022.112270

Ladd, C. C., and DeGroot, D. J. (2004). Recommended practice for soft ground site characterization: Arthur Casagrande Lecture. *Massachusetts Institute Technol.*

Lim, B., Tumay, M., and Seo, D. (2006). *Status of Consolidation From Incomplete Piezocone Dissipation Tests. Proceedings of Sessions of Geoshanghai: Site and Geomaterial Characterization* (Shanghai: ASCE), 56–63.

Liu, Z., and Xue, J. (2022). The deformation characteristics of a kaolin clay under intermittent cyclic loadings. *Soil Dynamics Earthquake Eng.* 153, 107112. doi: 10.1016/j.soildyn.2021

Liu, Z., Xue, J., and Mei, G. (2021). The impact of stress disturbance on undrained cyclic behaviour of a kaolin clay and settlement of tunnels under cyclic loading. *Acta Geotech.* 16, 3947–3961. doi: 10.1007/s11440-021-01363-x

Ma, C., Zhan, H. B., Zhang, T., and Yao, W. M. (2019). Investigation on shear behavior of soft interlayers by ring shear tests. *Eng. Geol.* 254, 34–42. doi: 10.1016/j.enggeo.2019.04.002

Martin, P. P., and Seed, H. B. (1983). One-dimensional dynamic ground response analyses. *J. Geotech. Eng. Division* 108, 935–952. doi: 10.1061/AJGEB6.0001316

Shan, Y., Lu, Z. R., Cui, J., Li, W., Li, Y. D., and Sun, W. X. (2024). Rheological study of the effect of marine clay mineral composition on nonlinear viscoelasticity. *Appl. Clay Sci.* 249, 107229. doi: 10.1016/j.clay.2023.107229

Sun, J., Yuan, X., and Sun, Y. (2004). Reasonability comparison between recommended and code values of dynamic shear modulus and damping ratio of soils. *Earthquake Eng. Eng. Vibration* 02), 125–133. doi: 10.3969/j.issn.1000-1301.2004.02.022

Tankiewicz, M. (2015). Experimental investigation of strength anisotropy of varved clay. *Proc. Earth Planet. Sci.* 15, 732–737. doi: 10.1016/j.proeps.2015.08.116

Tankiewicz, M. (2016). Structure investigations of layered soil-varved clay. *Ann. Warsaw Univ. Life Sci. SGGW* 48, 365–375. doi: 10.1515/sggw-2016-0028. Land Reclamation.

Wang, J., Du, X., Dai, M., Fu, H., Gao, Z., and Ni, J. (2025). Undrained cyclic behavior of marine soft clay considering different consolidated degrees in cyclic simple shear tests. *Soil Dynamics Earthquake Eng.* 196, 109480. doi: 10.1016/j.soildyn.2025.109480

Wang, Y., Lei, J., Wang, Y., and Li, S. (2019). Post-cyclic shear behavior of reconstituted marine silty clay with different degrees of reconsolidation. *Soil Dynamics Earthquake Eng.* 116, 530–540. doi: 10.1016/j.soildyn.2018.10.042

Wichtmann, T., and Triantafyllidis, T. (2017). Monotonic and cyclic tests on kaolin: A database for the development, calibration and verification of constitutive models for cohesive soils with focus to cyclic loading. *Acta Geotech.* 13, 1–26. doi: 10.1007/s11440-017-0588-3

Wong, J. K. H., Wong, S. Y., and Wong, K. Y. (2022). Extended model of shear modulus reduction for cohesive soils. *Acta Geotech.* 17, 2347–2363. doi: 10.1007/s11440-021-01398-0

Xiao, X., Guan, X., Wu, Q., Zhao, D. F., Zhou, R. R., and Chen, G. X. (2025). Energy-based method for the failure criterion and resistance evaluation of marine clay under cyclic loading. *Eng. Geol.* 344, 107833. doi: 10.1016/j.enggeo.2024.107833

Xiao, X., Ji, D. W., Hang, T. Z., Cai, Z. Y., Zhang, L., Wu, Q., et al. (2023). Cyclic threshold shear strain for pore water pressure generation and stiffness degradation in marine clays at Yangtze estuary. *Front. Mar. Sci.* 10, 1184225. doi: 10.3389/fmars.2023.1184225

Xiao, X., Wang, Z. F., Wu, Q., Zhou, R. R., and Chen, G. X. (2024). Shear-thinning non-Newtonian fluid-based method for investigating cyclic stiffness degradation of marine clay. *Ocean. Eng.* 300, 117499. doi: 10.1016/j.oceaneng.2024.117499

Yang, W. B., Wu, Q., and Chen, G. X. (2019). Dynamic shear modulus prediction method of undisturbed soil in the estuary of the Yangtze River. *Rock Soil Mechanics* 40, 3889–3896. doi: 10.16285/j.rsm.2019.0192

Zheng, J., Hu, X., Gao, S., Wu, L., Yao, S., Dai, M., et al. (2024). Undrained cyclic behavior of under-consolidated soft marine clay with different degrees of consolidation. *Mar. Georesources Geotechnol.* 42, 176–183. doi: 10.1080/1064119X.2022.2158766

Zhu, W., Wang, J., and Zhuang, H. (2022). Influence of cyclic deviator stress and consolidation degree on permanent strain of "under-consolidated" Marine sediment. *Mar. Georesources Geotechnol.* 41, 1–10. doi: 10.1080/1064119X.2022.2098888

Zhuang, H., Hu, X., Guo, L., et al. (2022). Effect of initial deviatoric stress on anisotropy of marine clay during principal stress rotation. *Mar. Georesources Geotechnol.* 40, 64–77. doi: 10.1080/1064119X.2020.1865489

Zhuang, H. Y., Yang, J., Chen, S., Li, H. X., Zhao, K., and Chen, G. X. (2020). Liquefaction performance and deformation of slightly sloping site in floodplains of the lower reaches of Yangtze River. *Ocean. Eng.* 217, 107869. doi: 10.1016/j.oceaneng.2020.107869